DOI: 10.1021/ma102230m

Macromolecules
ARTICLE

Stable Aqueous Dispersion of Graphene Nanosheets: Noncovalent Functionalization by a Polymeric Reducing Agent and Their Subsequent Decoration with Ag Nanoparticles for Enzymeless Hydrogen Peroxide Detection

Sen Liu,[†] Jingqi Tian,[†,‡] Lei Wang,[†] Hailong Li,[†] Yingwei Zhang,[†] and Xuping Sun*[,†]

[†]*State Key Lab of Electroanalytical Chemistry, Changchun Institute of Applied Chemistry, Chinese Academy of Sciences, Changchun 130022, Jilin, China, and* [‡]*Graduate School of the Chinese Academy of Sciences, Beijing 100039, China*

Received September 28, 2010; Revised Manuscript Received November 5, 2010

ABSTRACT: An aqueous dispersion of graphene nanosheets (GNs) has been successfully prepared via chemical reduction of graphene oxide (GO) by hydrazine hydrate in the presence of poly[(2-ethyldimethylammonioethyl methacrylate ethyl sulfate)-*co*-(1-vinylpyrrolidone)] (PQ11), a cationic polyelectrolyte, for the first time. The noncovalent functionalization of GN by PQ11 leads to a GN dispersion that can be very stable for several months without the observation of any floating or precipitated particles. Several analytical techniques including UV−vis spectroscopy, Raman spectroscopy, X-ray diffraction (XRD), and X-ray photoelectron spectroscopy (XPS) have been used to characterize the resulting GNs. Taking advantages of the fact that PQ11 is a positively charged polymer exhibiting reducing ability, we further demonstrated the subsequent decoration of GN with Ag nanoparticles (AgNPs) by two routes: (1) direct adsorption of preformed, negatively charged AgNPs; (2) in-situ chemical reduction of silver salts. It was found that such Ag/GN nanocomposites exhibit good catalytic activity toward the reduction of hydrogen peroxide (H_2O_2), leading to an enzymeless sensor with a fast amperometric response time of less than 2 s. The linear detection range is estimated to be from 100 μM to 40 mM ($r = 0.996$), and the detection limit is estimated to be 28 μM at a signal-to-noise ratio of 3.

Introduction

Since the discovery by Novoselov et al.,[1] graphene, a flat monolayer of sp^2-bonded carbon atoms tightly packed into a two-dimensional (2D) honeycomb lattice, and characterized as "the thinnest material in our universe",[2−4] has received considerable attention due to its high surface area (~2600 m^2/g), high chemical stability, and unique electronic and mechanical properties,[5] which ensure its potential applications in nanoelectronics,[6] nanocomposites,[7] Li ion batteries,[8] and sensors.[9] The first challange for the practical applications of graphene is its processing of graphene nanosheet (GN).[2] A prerequisite for exploiting most applications for graphene is the availability of processable GNs in large quantities, and thus the development of efficient and cost-effective approaches to producing processable GNs on a large scale has been paid considerable attention. Up to now, numerous techniques such as micromechanical exfoliation,[1] chemical vapor deposion,[10,11] chemical reduction of graphene oxide (GO),[12,13] electrochemical reduction of GO,[14] photoreduction of GO,[15−18] and other special stratagies,[19−22] etc., have been successfully developed for synthesis of GNs. Among them, the chemical reduction of GO holds the great advantage of low cost and bulk quantity production.[23−25] Currently, hydrazine and hydrazine hydrate exihibit much higher reduction degree than other chemicals and hence are widely used for reduction of GO, resulting in significantly loss oxygen-containing functional groups and restoration of much of the $\pi-\pi$ conjugation.[12,24,26−28] Unfortunately, the GNs thus formed readily form irreversible aggregates in water due to the strong van der Waals interactions between them.[29]

Recently, numerous approaches have been successfully developed to prepare stable aqueous dispersion of GNs by chemical reduction of GO with hydrazine. For example, the pH-control reduction process has been proven to be a successful route to obtain stable GN dispersion through electrostatic stabilization.[12,30] Additionally, it is demonstrated that organic polymers and surfactants such as pyrene butyrate,[24] ssDNA,[31] poly(sodium 4-styrenesulfonate),[25] methylene green,[32] Nafion,[33] Congo red,[34] ionic liquid polymer,[35] polyvinylpyrrolidone (PVP),[36] sulfonated polyaniline,[37] pluronic copolymer,[38] 7,7,8,8-tetracyanoquinodimethane,[39] and chitosan[40] are capable of stabilizing GN by decreasing the van der Waals interactions between the reduced GO nanosheets. Meanwhile, organic solvents such as *N,N*-dimethylformamide[41−44] and *N*-methylpyrrolidone[45] have also been used to prepare stable GNs dispersion due to strong interactions between solvent molecules and graphene. Although there are many papers dealing with the use of polymers to stabilize GNs, the noncovalent functionalization of GNs by a polymeric reducing agent and their subsequent decoration of such GNs by metal nanoparticles by in-situ chemical reduction of metal salts have not addressed so far.

In this paper, as a polymeric reducing agent and cationic polyelectrolyte PQ11 (see Figure S1 for chemical structure) is used as a stabilizing agent for GNs in water for the first time. We further demonstrate the subsequent decoration of the resulting GN with Ag nanoparticles (AgNPs) by two routes: (1) direct adsorption of preformed, negatively charged AgNPs; (2) in-situ

*To whom correspondence should be addressed: Fax 0086-431-85262065; e-mail sunxp@ciac.jl.cn.

 Published on Web 11/17/2010

chemical reduction of silver salts. It was found that such Ag/GN nanocomposites exhibit good catalytic activity toward the reduction of hydrogen peroxide (H_2O_2), leading to an enzymeless sensor with a fast amperometric response time of less than 2 s. The linear detection range is estimated to be from 100 μM to 40 mM ($r = 0.996$), and the detection limit is estimated to be 28 μM at a signal-to-noise ratio of 3.

Experimental Section

Chemicals. PQ11, graphite powder, $AgNO_3$, NaH_2PO_4, Na_2HPO_4, and H_2O_2 (30%) were purchased from Aladin Ltd. (Shanghai, China). $NaNO_3$, sodium citrate, H_2SO_4 (98%), and $KMnO_4$ were purchased from Beijing Chemical Corp. Hydrazine hydrate and sodium borohydride ($NaHB_4$) were purchased from Tianjin Fuchen Chemical Corp. All chemicals were used as received without further purification. The water used throughout all experiments was purified through a Millipore system. Phosphate buffer saline (PBS) was prepared by mixing stock solutions of NaH_2PO_4 and Na_2HPO_4, and a fresh solution of H_2O_2 was prepared daily.

Apparatus. UV−vis spectra were obtained on a UV5800 spectrophotometer. Raman spectra were obtained on J-Y T64000 Raman spectrometer with 514.5 nm wavelength incident laser light. Powder X-ray diffraction (XRD) data were recorded on a Rigaku D/MAX 2550 diffractometer with Cu Kα radiation ($\lambda = 1.5418$ Å). X-ray photoelectron spectroscopy (XPS) analysis was measured on an ESCALAB MK II X-ray photoelectron spectrometer using Mg as the exciting source. Transmission electron microscopy (TEM) measurements were made on a Hitachi H-8100 electron microscope (Hitachi, Tokyo, Japan) with an accelerating voltage of 200 kV. The sample for TEM characterization was prepared by placing a drop of colloidal solution on carbon-coated copper grid and dried at room temperature.

Preparation of GO. GO was prepared from natural graphite powder through a modified Hummers' method.[23] In a typical synthesis, 1 g of graphite was added into 23 mL of 98% H_2SO_4, followed by stirring at room temperature over a 24 h period. After that, 100 mg of $NaNO_3$ was introduced into the mixture and stirred for 30 min. Subsequently, the mixture was kept below 5 °C by ice bath, and 3 g of $KMnO_4$ was slowly added into the mixture. After being heated to 35−40 °C, the mixture was stirred for another 30 min. After that, 46 mL of water was added into above mixture during a period of 25 min. Finally, 140 mL of water and 10 mL of 30% H_2O_2 were added into the mixture to stop the reaction. After the unexploited graphite in the resulting mixture was removed by centrifugation, as-synthesized GO was dispersed into individual sheets in distilled water at a concentration of 0.5 mg/mL with the aid of ultrasound for further use.

Preparation of GNs. In a typical synthesis, 3 mL of GO aqueous dispersion was added into 1 mL of H_2O, followed by addition of 1 mL of PQ11 (0.8 mol/L) and 1 mL of hydrazine hydrate aqueous (0.1 mol/L). After stirring for 30 min at room temperature, the mixture was heated to 100 °C over a 1 h period. Finally, a black GN dispersion with a concentration of 0.25 mg/mL was obtained. The excess PQ11 and hydrazine were removed by centrifugation twice, and the resulting precipitates were redispersed in water for characterization and further use.

Preparation of Ag/GN Nanocomposites. In the present study, two different methods were used to prepare Ag/GN nanocomposites. (1) The nanocomposites were prepared by adsorption of citrate-stabilized AgNPs onto the resulting PQ11-stabilized GN (designated as Ag/GN-A). AgNPs with a concentration of 0.4 mM were prepared via reduction of $AgNO_3$ by $NaHB_4$ with the use of sodium citrate as a stabilizing agent at room temperature. In a typical preparation of Ag/GN-A, 1 mL of GN dispersion was mixed with 1 mL of AgNPs aqueous solution first, and then the mixture was sonicated for 2 min. After that, the mixture was placed at room temperature over a 12 h period. Finally, the precipitate was collected by centrifugation and washed with water twice and then redispersed in 0.5 mL of H_2O for characterization and further use. (2) The nanocomposites were prepared by in-situ reduction of $AgNO_3$ by PQ11 (designated as Ag/GN-R). In a typical preparation, 10 μL of $AgNO_3$ (0.5 mol/L) was added into 1 mL of GN dispersion first, and then the mixture was heated at 100 °C over a 30 min period. The precipitate was collected by centrifugation and washed with water twice and then redispersed in 0.5 mL of H_2O for characterization and further use.

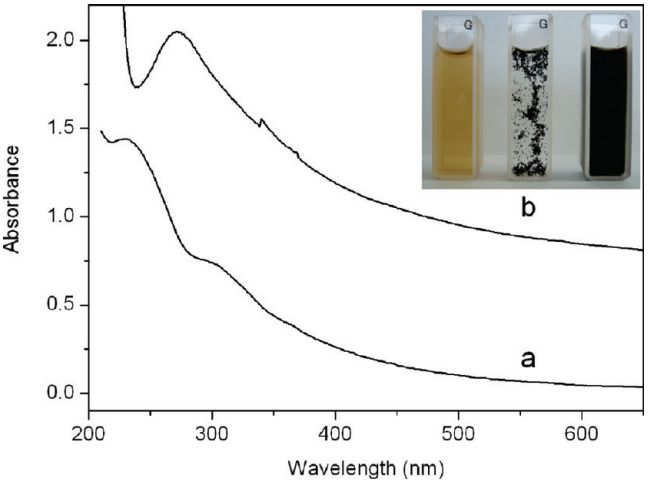

Figure 1. UV−vis spectra of aqueous dispersion of GO and the resulting GNs. Inset: photographs of aqueous dispersions of GO (left), GNs reduced by hydrazine hydrate in the absence of PQ11 (middle), and GNs reduced by hydrazine hydrate in the presence of PQ11 (right).

Electrochemical Measurements. Electrochemical measurements are performed with a CHI 660D electrochemical analyzer (CH Instruments, Inc., Shanghai). A conventional three-electrode cell was used, including a glassy carbon electrode (geometric area = 0.07 cm^2) as the working electrode, a Ag/AgCl (saturated KCl) electrode as the reference electrode, and platinum foil as the counter electrode. The potentials are measured with a Ag/AgCl electrode as the reference electrode. All the experiments were carried out at ambient temperature.

Results and Discussion

Figure 1 shows the UV−vis spectra of aqueous dispersion of GO and the resulting GNs. As expected, GO exhibits strong bands centered at 230 and 300 nm, corresponding to $\pi \rightarrow \pi^*$ transitions of aromatic C=C band and n $\rightarrow \pi^*$ transitions of C=O band in GO, respectively, as shown in Figure 1a.[46] It is clearly seen that the adsorption peak gradually red-shifts from 230 to 270 nm, and the absorbance in the whole spectral region increases after heat treatment. Such observations suggest that the electronic conjugation within the GO is restored upon the heat treatment.[46] Figure 1 inset shows photographs of aqueous dispersion of GO (left) and the resulting GNs (right), revealing a distinct color change from pale-yellow to black after heat treatment. Such an observation provides another piece of evidence to support the formation of GNs.[47] It is worthwhile mentioning that the GNs dispersion thus formed can be well-stable for several months without the observation of any floating or precipitate particles, indicating PQ11 serves as an effective stabilizing agent for GNs which could be attributed that the cationic PQ11 is capable of combining both steric and electrostatic stabilization, resulting in electrosteric stabilization. In contrast, GNs otained in the absence of PQ11 form aggregates more readily and rapidly than PQ11-stabilized GNs. The excellent stability of the GNs in our present study can be reasoned as follows: The PVP segments along PQ11 chain have great affinity to the graphite surface,[48]

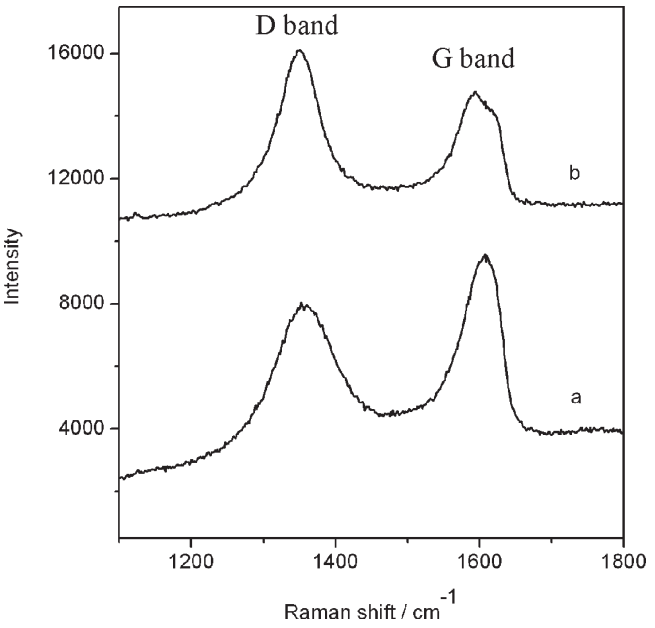

Figure 2. Raman spectra of GO (a) and GNs (b).

and thus PQ11 chains are strongly attached to and noncovalently functionalize the GN surfaces.[36] On the other hand, PQ11 is a kind of cationic polyelectrolyte, and thus the cationic adlayers confer to the GN both the steric and electrostatic repulsions, resulting in electrosteric stabilization. The combination of these two attributes together with the multipoint attachment of the PQ11 chain contributes to the formation of GNs with remarkable colloidal stability.

The formation of GNs is also evidenced by the corresponding Raman spectra. Figure 2 shows the Raman spectra of GO and as-formed GNs. It is established that graphene obtained by chemical reduction of GO exhibits two characteristic main peaks: the D band at ~1350 cm^{-1}, arising from a breathing mode of κ-point photons of A_{1g} symmetry; the G band at 1575 cm^{-1}, arising from the first order scattering of the E_{2g} phonon of sp^2 C atoms.[49] In our present study, it is seen that GO exhibits a D band at 1350 cm^{-1} and a G band at 1603 cm^{-1}, while the corresponding bands of GNs are 1350 and 1593 cm^{-1}, respectively. The G band of GNs red-shifts from 1603 to 1593 cm^{-1}, which is atributed to the high ability for recovery of the hexagonal network of carbon atom.[50] It is also found that GNs show relative higher intensity of D to G band than that of GO. These observations further confirm the formation of new graphitic domains after the heat treatment process.[51]

Figure 3 shows the XRD patterns of GO and GNs. Graphite powder (Figure S2) shows a sharp (002) peak at 26.4° with a typical interspacing of 3.35 Å. However, it is found that GO (Figure 3a) exhibits a strongly peak at 10.02° corresponding to the (002) interplanar spacing of 8.2 Å, which suggests that graphite has been successfully oxidized by Hummers' method. It is also seen that the corresponding peak disappears after the heat treatment process (Figure 3b), indicating the successful reduction of GO.

Survey X-ray photoelectron spectroscopy is a significant measure to observe the inner strucutre of C for carbon-based materials. It is well kown that the bands centered at 284.8 and 531.0 eV are associated with C 1s and O 1s, respectively. It is clearly seen that the O 1s intensity of GNs is significantly decreased compared with that of GO, suggesting the loss of oxygen in GO after the heat treatment (Figure S3). The new peak at 400.0 eV associated with N 1s was observed, which can be attributed to the presence of nitrogen element in the PQ11, indicating the adsorption of PQ11 on GNs. Figure 4 shows the C 1s XPS spectra of GO and GNs. The C 1s spectra of GO and

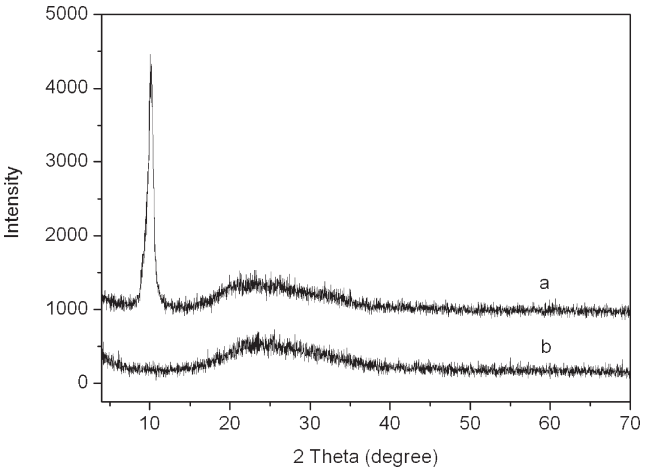

Figure 3. XRD patterns of GO (a) and GNs (b).

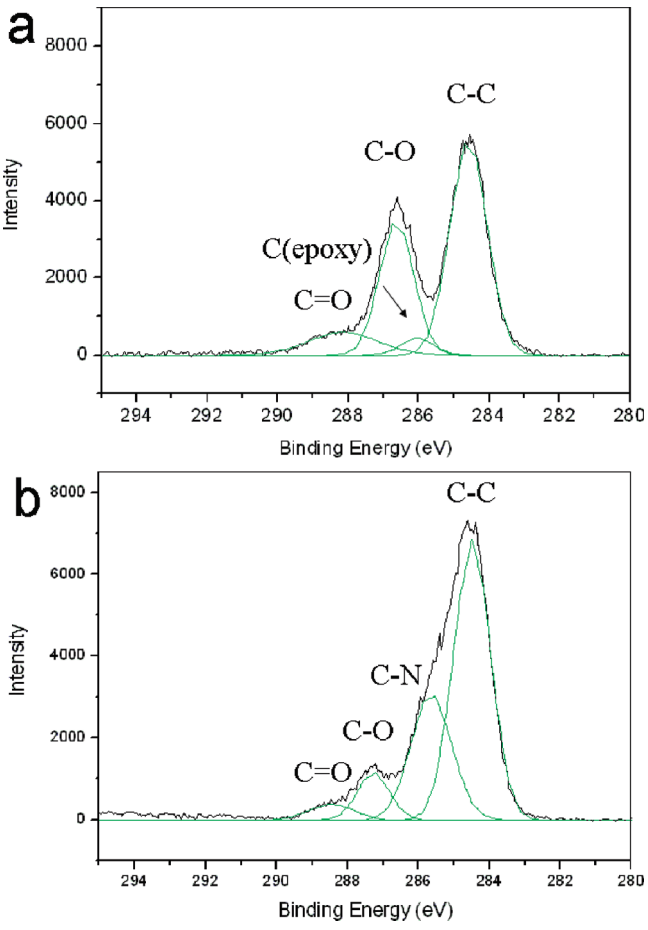

Figure 4. C 1s XPS spectra of GO (a) and GNs (b).

GNs could be deconvoluted into four peaks at 284.5, 285.6, 286.6, and 288.4 eV, which are associated with C−C, C−OH, C (epoxy/alkoxy), and C=O, respectively.[30] It is obviously seen that the peak intensity of C−O and C=O in strong in GO (Figure 4a). In contrast, after the heat treatment process, the peak intensity of C−O and C=O in GNs (Figure 4b) tremendously decreases, and the content of C−C correspondingly increases dramatically. In addition, it is also seen that a new peak at 286 eV is observed, further confirming the presence of PQ11. All the observations suggest that the most oxygen-containing functional groups are successfully removed after heat treatment process.

Scheme 1. Illustration (Not to Scale) of the Reduction of GO to GNs Noncovalently Functionalized by PQ11 and the Subsequent Preparation of Ag/GN Nanocomposites through Two Different Routes

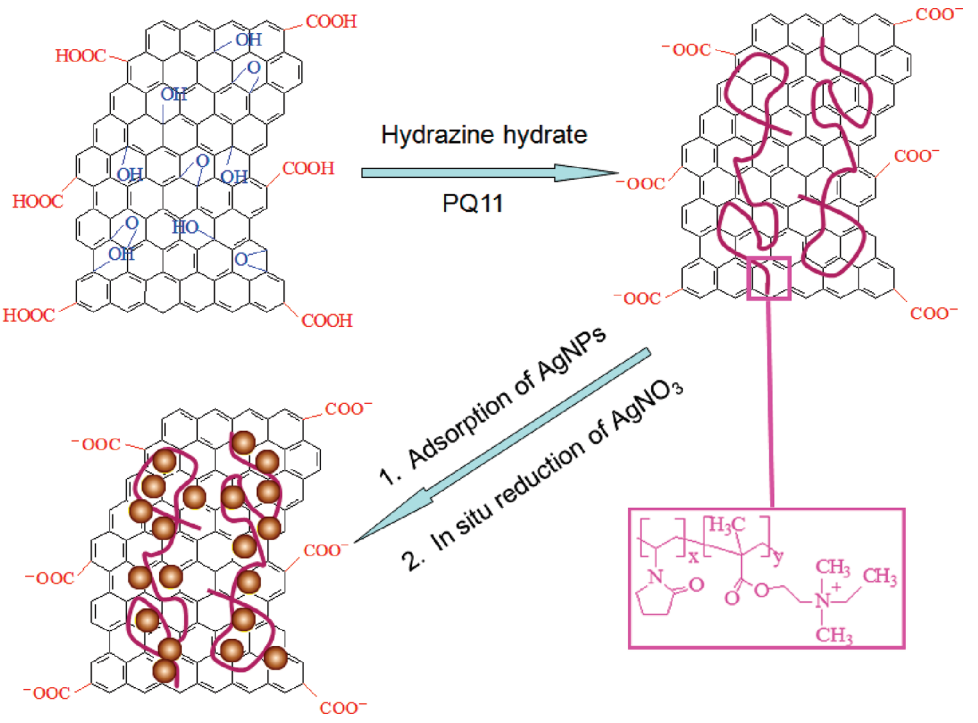

Because PQ11 is a positively charged polymer exhibiting reducing ability, it is expected that the resulting GN can be easily decorated with nanoparticles via direct adsorption of preformed, negatively charged nanoparticles or in-situ chemical reduction of metal salts. It is also well-known that AgNPs exhibit high catalytic activity for H_2O_2 reduction.[52,53] Furthermore, Ag/GN nanocomposites and the their applications have attracted much attention during the past few years.[54−56] Thus, we demonstrated the proof of concept of preparing Ag/GN nanocomposites by two different routes and their application for enzymeless H_2O_2 detection. Scheme 1 presents a scheme (not to scale) to illustrate the reduction of GO to GNs noncovalently functionalized by PQ11 and the subsequent preparation of Ag/GN nanocomposites through two different routes. First, GN dispersion was obtained via chemical reduction of GO by hydrazine hydrate using PQ11 as a stabilizing agent. Second, two different routes are used to prepare Ag/GN nanocomposites: (1) direct adsorption of preformed, negatively charged AgNPs stabilized by citrate based on the positively charged nature of PQ11 chain (designated as Ag/GN-A); (2) in-situ chemical reduction of silver salts based on the inherent reducing ability of PVP segments (designated as Ag/GN-R).[57] Figure 5 shows the typical TEM images of the nanocomposites. It is clearly seen that the direct adsorption method results in the formation of GNs decorated with a large amount of AgNPs, as shown in Figure 5a. On the other hand, in-situ chemical reduction method leads to small AgNPs which are uniformly and exclusively absorbed on the GN substrate, as shown in Figure 5b. All these observations provide clear evidence to support the formation of Ag/GN nanocomposites. We also performed one control experiment where AgNPs were directly adsorbed on GN with the absence of PQ11. The corresponding TEM image of the resultant products indicates that the amount of AgNPs attached on GN decreases dramatically, as shown in Figure S4. All the above observations show that PQ11 makes a great contribution to the AgNPs adsorption.

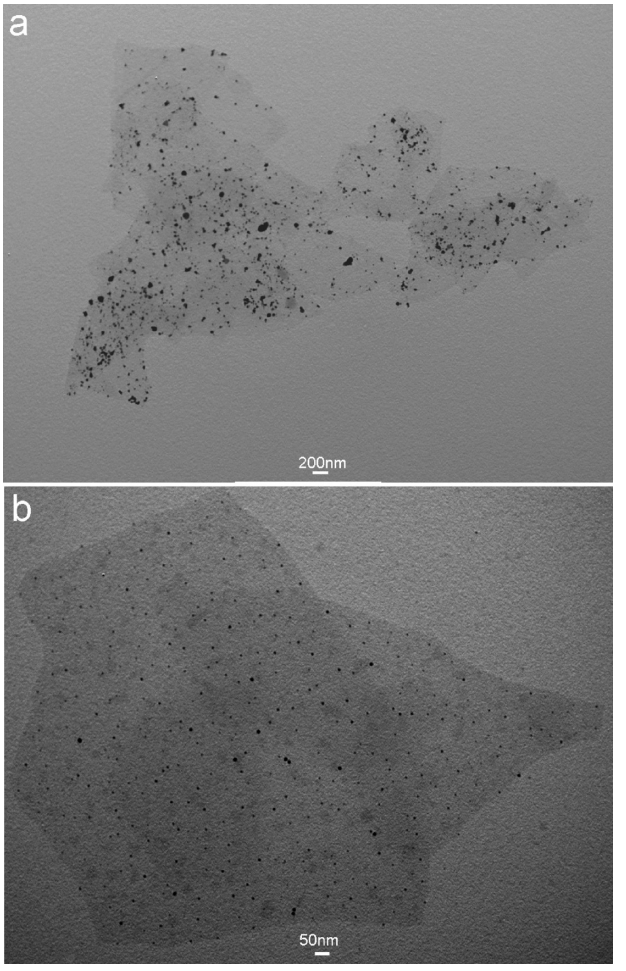

Figure 5. TEM image of Ag/GN-A (a) and Ag/GN-R (b).

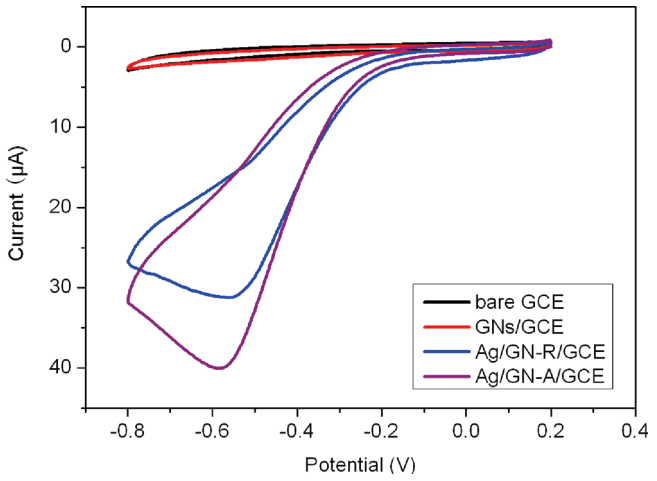

Figure 6. Cyclic voltammetry (CVs) of a bare GCE, GNs/GCE, Ag/GN-R/GCE, and Ag/GN-A/GCE in N_2 saturated 0.2 M PBS at pH 6.5 in the presence of 1.0 mM H_2O_2 (scan rate: 0.02 V/s).

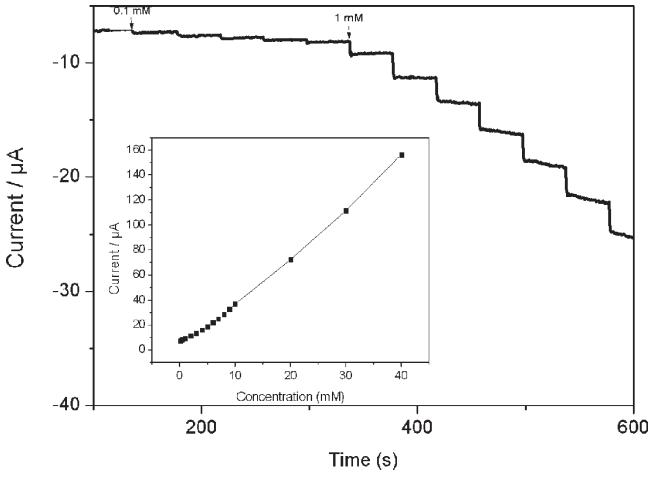

Figure 7. Typical steady-state response of the Ag/GN-R/GCE to successive injection of H_2O_2 into the N_2 saturated PBS under stirring. The inset was the calibration curve. Applied potential: −0.40 V; supporting electrolyte: 0.2 M PBS of pH 6.5.

As a demonstration of application of such nanocomposites, we constructed an enzymeless H_2O_2 sensor by direct deposition of the aqueous dispersion of Ag/GN nanocomposites on a bare glassy carbon electrode (GCE) surface. Figure 6 shows the electrocatalytic responses of a bare GCE, GNs modified GCE (designated as GNs/GCE), and Ag/GN-R and Ag/GN-A modified GCE (designated as Ag/GN-R/GCE and Ag/GN-A/GCE, respectively) in N_2 saturated 0.2 M PBS at pH 6.5 in the presence of 1.0 mM H_2O_2 (scan rate: 0.02 V/s). Obviously, the response of both the bare GCE and the GNs/GCE toward the reduction of H_2O_2 is pretty weak. In contrast, it is seen that Ag/GN-R and Ag/GN-A exhibit a remarkable catalytic current peak about 30 μA in intensity at −0.54 V and about 40 μA in intensity at −0.58 V, respectively. All these observations reveal that the AgNPs exhibit notable catalytic ability for H_2O_2 reduction. Compared to Ag/GN-R/GCE, the Ag/GN-A exhibits a 33% enhancement of peak current and a 0.04 V negative shift of the peak potential. It could be attributed to the higher loading and larger particle size of AgNPs, as is evidenced by the TEM observations (Figure 5).

Figure 7 shows the typical current−time plot of the Ag/GN-R/GCE in N_2-saturated 0.2 M PBS buffer (pH: 6.5) on successive step change of H_2O_2 concentrations under optimized conditions. When an aliquot of H_2O_2 was added into the stirring PBS solution, Ag/GN-R/GCE responded rapidly to the substrate and the current rose steeply to reach a stable value. At the applied potential of −0.40 V, the cathode current of the sensor increased dramatically and achieved 95% of the steady state current within 2 s, revealing a fast amperometric response behavior. The inset shows the calibration curve of the sensor. The linear detection range is estimated to be from 100 μM to 40 mM (r = 0.996), and the detection limit is estimated to be 28 μM at a signal-to-noise ratio of 3.

Conclusions

In summary, chemical reduction of GO in the presence of PQ11 has been proven to be an effective method for the preparation of well-stable aqueous dispersion of GNs. Both the electrosteric stabilization and the multipoint attachment of the PQ11 chain to the GN surface are responsible for its remarkable colloidal stability of the GN dispersion. Taking advantage of the fact that PQ11 is a cationic polyelectrolyte exhibiting reducing ability, we have successfully demonstrated the decoration of GN with AgNPs via direct adsorption of preformed, negatively charged AgNPs or in-situ chemical reduction of silver salts. The detection of H_2O_2 without using enzyme in the electrode modified by Ag/GN nanocomposites has also been demonstrated, and it revealed that the AgNPs contained therein exhibit notable catalytic activity toward the reduction of H_2O_2. Our present findings provide us a low-cost approach to the facile production of stable aqueous dispersions of GNs and nanoparticles/GNs composites on a large scale for applications.

Acknowledgment. This work was supported by National Basic Research Program of China (No. 2011CB935800).

Supporting Information Available: Chemical structure of PQ11; XRD pattern of natural graphite; XPS spectra of GO and GNs; TEM image of Ag/GN obtained in the absence of PQ11. This material is available free of charge via the Internet at http://pubs.acs.org.

References and Notes

(1) Geim, A. K.; Novoselov, K. S. *Nature Mater.* **2007**, *6*, 183.
(2) Novoselov, K. S.; Geim, S. V.; Morozov, S. V.; Jiang, D.; Zhang, Y.; Dubonos, S. V.; Grigorieva, I. V.; Firsov, A. A. *Science* **2004**, *306*, 666.
(3) Allen, M. J.; Tung, V. C.; Kaner, R. B. *Chem. Rev.* **2010**, *110*, 132.
(4) Rao, C. N. R.; Sood, A. K.; Subrahmanyam, K. S.; Govindaraj, A. *Angew. Chem., Int. Ed.* **2009**, *48*, 7752.
(5) Dikin, D. A.; Stankovich, S.; Zimney, E. J.; Piner, R. D.; Dommett, G. H. B.; Evmenenko, G.; Nguyen, S. T.; Ruoff, R. S. *Nature* **2007**, *448*, 457.
(6) Zhang, Y.; Tan, Y.-W.; Stormer, H. L.; Kim, P. *Nature* **2005**, *438*, 201.
(7) Stankovich, S.; Dikin, D. A.; Dommett, G. H. B.; Kohlhaas, K. M.; Zimney, E. J.; Stach, E. A.; Piner, R. D.; Nguyen, S. T.; Ruoff, R. S. *Nature* **2006**, *442*, 282.
(8) Yoo, E.; Kim, J.; Hosono, E.; Zhou, H.-S.; Kudo, T.; Homa, I. *Nano Lett.* **2008**, *8*, 2277.
(9) Shan, C.; Yang, H.; Song, J.; Han, D.; Ivaska, A.; Niu, L. *Anal. Chem.* **2009**, *81*, 5603.
(10) Land, T. A.; Michely, T.; Behm, R. J.; Hemminger, J. C.; Comsa, G. *Surf. Sci.* **1992**, *264*, 261.
(11) Kim, K. S.; Zhao, Y.; Jang, H.; Lee, S. Y.; Kim, J. M.; Kim, K. S.; Ahn, J.-H.; Kim, P.; Choi, J.-Y.; Hong, B. H. *Nature* **2009**, *457*, 706.
(12) Li, D.; Müller, M. B.; Gilje, S.; Kaner, R. B.; Wallace, G. G. *Nature Nanotechnol.* **2008**, *3*, 101.
(13) Wang, H.; Robinson, J. T.; Li, X.; Dai, H. *J. Am. Chem. Soc.* **2009**, *131*, 9910.
(14) Wang, Z.; Zhou, X.; Zhang, J.; Boey, F.; Zhang, H. *J. Phys. Chem. C* **2009**, *113*, 14071.

(15) Zhang, Y.; Guo, L.; Wei, S.; He, Y.; Xia, H.; Chen, Q.; Sun, H.-B.; Xiao, F.-S. *Nano Today* **2010**, *5*, 15.
(16) Williams, G.; Seger, B.; Kamat, P. V. *ACS Nano* **2008**, *2*, 1487.
(17) Williams, G.; Kamat, P. V. *Langmuir* **2009**, *25*, 13869.
(18) Li, H.; Pang, S.; Peng, X.; Müllen, K.; Bubeck, C. *Chem. Commun.* **2010**, *46*, 6243.
(19) Zhu, Y.; Murali, S.; Stoller, M. D.; Velamakanni, A.; Piner, R. D.; Ruoff, R. S. *Carbon* **2010**, *48*, 2106.
(20) Zhang, W.; Cui, J.; Tao, C.-A.; Wu, Y.; Li, Z.; Ma, L.; Wen, Y.; Li, G. *Angew. Chem., Int. Ed.* **2009**, *48*, 5864.
(21) Kosynkin, D. V.; Higginbotham, A. L.; Sinitskii, A.; Lomeda, J. R.; Dimiev, A.; Price, B. K.; Tour, J. M. *Nature* **2009**, *458*, 872.
(22) Jiao, L.; Zhang, L.; Wang, R.; Diankov, G.; Dai, H. *Nature* **2009**, *458*, 877.
(23) Hummers, W. S., Jr; Offeman, R. *J. Am. Chem. Soc.* **1958**, *80*, 1339.
(24) Xu, Y.; Bai, H.; Lu, G.; Li, C.; Shi, G. Q. *J. Am. Chem. Soc.* **2008**, *130*, 5856.
(25) Stankovich, S.; Piner, R. D.; Chen, X.; Wu, N.; Nguyen, S. T.; Ruoff, R. S. *J. Mater. Chem.* **2006**, *16*, 155.
(26) Tung, V. C.; Allen, M. J.; Yang, Y.; Kaner, R. B. *Nature Nanotechnol.* **2009**, *4*, 25.
(27) Higginbotham, A. L.; Kosynkin, D. V.; Sinitskii, A.; Sun, Z.; Tour, J. M. *ACS Nano* **2010**, *4*, 2059.
(28) Jiang, B.; Tian, C.; Wang, L.; Xu, Y.; Wang, R.; Qiao, Y.; Ma, Y.; Fu, H. *Chem. Commun.* **2010**, *46*, 4920.
(29) Stankvich, S.; Dikin, D. A.; Piner, R. D.; Kohlhaas, K. A.; Kleinhammes, A.; Jia, Y.; Wu, Y.; Nguyen, S. T.; Ruoff, R. S. *Carbon* **2007**, *45*, 1558.
(30) Park., S.; An, J.; Piner, R. D.; Jung, I.; Yang, D.; Velamakanni, A.; Nguyen, S. T.; Ruoff, R. S. *Chem. Mater.* **2008**, *20*, 6592.
(31) Patil, A. J.; Vickery, J. L.; Scott, T. B.; Mann, S. *Adv. Mater.* **2009**, *21*, 3159.
(32) Liu, H.; Gao, J.; Xue, M.; Zhu, N.; Zhang, M.; Cao, T. *Langmuir* **2009**, *25*, 12006.
(33) Choi, B. G.; Park, H.; Park, T. J.; Yang, M. H.; Kim, J. S.; Jang, S.-Y.; Heo, N. S.; Lee, S. Y.; Kong, J.; Hong, W. H. *ACS Nano* **2010**, *4*, 2910.
(34) Li, F.; Bao, Y.; Chai, J.; Zhang, Q.; Han, D.; Niu, L. *Langmuir* **2010**, *26*, 12314.
(35) Kim, T.; Lee, H.; Kim, J.; Suh, K. S. *ACS Nano* **2010**, *4*, 1612.
(36) Bourlinos, A. B.; Georgakilas, V.; Zboril, R.; Steriotis, T. A.; Stubos, A. K.; Trapalis, C. *Solid State Commun.* **2009**, *149*, 2172.
(37) Bai, H.; Xu, Y.; Zhao, L.; Li, C.; Shi, G. *Chem. Commun.* **2009**, 1667.
(38) Zu, S.-Z.; Han, B.-H. *J. Phys. Chem. C* **2009**, *113*, 13651.
(39) Hao, R.; Qiao, W.; Zhang, L.; Hou, Y. *Chem. Commun.* **2008**, 6576.
(40) Zhou, Y.; Liu, S.; Jiang, H.; Yang, H.; Chen, H. *Electroanalysis* **2010**, *22*, 1323.
(41) Park., S.; An, J.; Jung, I.; Piner, R. D.; An, S. J.; Li, X.; Velamakanni, A.; Ruoff, R. S. *Nano Lett.* **2009**, *9*, 1593.
(42) Liang, Y.; Wu, D.; Feng, X.; Müllen, K. *Adv. Mater.* **2009**, *21*, 1679.
(43) Lomeda, J. R.; Doyle, C. D.; Kosynkin, D. V.; Hwang, W.-F.; Tour, J. M. *J. Am. Chem. Soc.* **2008**, *130*, 16201.
(44) Villar-Rodil, S.; Paredes, J. I.; MartÍnez-Alonso, A.; Tascón, J. M. D. *J. Mater. Chem.* **2009**, *19*, 3591.
(45) Hernandez, Y.; Nicolosi, V.; Lotya, M.; Blighe, F. M.; Sun, Z.; De, S.; McGovern, I. T.; Holland, B.; Byrne, M.; Gun'ko, Y. K.; Boland, J. J.; Niraj, P.; Duesberg, G.; Krishnamurthy, S.; Goodhue, R.; Hutchison, J.; Scardaci, V.; Ferrari, A. C.; Coleman, J. N. *Nature Nantechnol.* **2008**, *3*, 563.
(46) Guo, Y.; Guo, S.; Ren, J.; Zhai, Y.; Dong, S.; Wang, E. *ACS Nano* **2010**, *4*, 4001.
(47) Guo, S.; Wen, D.; Zhai, Y.; Dong, S.; Wang, E. *ACS Nano* **2010**, *4*, 3959.
(48) Otsuka, H.; Esumi, K. *J. Colloid Interface Sci.* **1995**, *170*, 113.
(49) Gao, J.; Liu, F.; Ma, N.; Wang, Z.; Zhang, X. *Chem. Mater.* **2010**, *22*, 2213.
(50) Li, Z.; Yao, Y.; Lin, Z.; Moon, K.-S.; Lin, W.; Wong, C. *J. Mater. Chem.* **2010**, *20*, 4781.
(51) Pimenta, M. A.; Dresselhaus, G.; Dresselhaus, M. S.; Cancado, L. G.; Jorio, A.; Saito, R. *Phys. Chem. Chem. Phys.* **2007**, *9*, 1276.
(52) Welch, C.; Banks, C.; Simm, A.; Compton, R. *Anal. Bioanal. Chem.* **2005**, *382*, 12.
(53) Song, Y.; Cui, K.; Wang, L.; Chen, S. *Nanotechnology* **2009**, *20*, 105501.
(54) Lu, G.; Mao, S.; Park, S.; Ruoff, R. S.; Chen, J. *Nano Res.* **2009**, *2*, 192.
(55) Lightcap, I. V.; Kosel, T. H.; Kamat, P. V. *Nano Lett.* **2010**, *10*, 577.
(56) Zhou, X.; Huang, X.; Qi, X.; Wu, S.; Xue, C.; Boey, F. Y. C.; Yan, Q.; Chen, P.; Zhang, H. *J. Phys. Chem. C* **2009**, *113*, 10842.
(57) Lim, B.; Camargo, P. H. C.; Xia, Y. *Langmuir* **2008**, *24*, 10437.